Nordenman, B., Nyström, C., & Björk, I. (1977) *Eur. J. Biochem. 78*, 195–203.
Owen, W. G. (1984) in *Biology of Endothelial Cells* (Jaffe, E. A., Ed.) pp 259–267, Martinus Nijhoff Publishers, Boston.
Owen, W. G., & Esmon, C. T. (1981) *J. Biol. Chem. 256*, 5532–5535.
Pearson, J. D., & Gordon, J. L. (1979) *Nature (London) 281*, 384–386.
Preissner, K. T., Wassmuth, R., & Müller-Berghaus, G. (1985) *Biochem. J. 231*, 349–355.
Salem, H. H., Maruyama, I., Ishii, H., & Majerus, P. W. (1984) *J. Biol. Chem. 259*, 12246–12251.
Shimada, K., & Ozawa, T. (1985) *J. Clin. Invest. 75*, 1308–1316.
Stenflo, J. (1976) *J. Biol. Chem. 251*, 355–363.
Stern, D., Nawroth, P., Marcum, J., Handley, D., Kisiel, W., Rosenberg, R. D., & Stern, K. (1985) *J. Clin. Invest. 75*, 272–279.
Suzuki, K., Kusumoto, H., & Hashimoto, S. (1986) *Biochim. Biophys. Acta 882*, 343–352.
Thiel, W., Preissner, K. T., Delvos, U., & Müller-Berghaus, G. (1986) *Blut 52*, 169–177.
Tollefsen, D. M., Majerus, D. W., & Blank, M. K. (1982) *J. Biol. Chem. 257*, 2162–2169.
Towbin, H., Staehelin, T., & Gordon, J. (1979) *Proc. Natl. Acad. Sci. U.S.A. 76*, 4350–4354.
Walker, F. J., Sexton, P. W., & Esmon, C. T. (1979) *Biochim. Biophys. Acta 571*, 333–342.
Weksler, B. B., Ley, C. W., & Jaffe, E. A. (1978) *J. Clin. Invest. 62*, 923–930.
Yin, E. T., Wessler, S., & Stoll, P. J. (1971) *J. Biol. Chem. 246*, 3703–3711.

Nucleation of Actin Polymerization by Villin and Elongation at Subcritical Monomer Concentration†

Annemarie Weber,*,‡ Jennifer Northrop,‡ Marilyn F. Bishop,§,‖ Frank A. Ferrone,§ and Mark S. Mooseker⊥
Pennsylvania Muscle Institute, University of Pennsylvania, Philadelphia, Pennsylvania 19104, Department of Physics and Atmospheric Science, Drexel University, Philadelphia, Pennsylvania 19104, and Department of Biology, Yale University, New Haven, Connecticut 06511

Received January 6, 1986; Revised Manuscript Received December 4, 1986

ABSTRACT: We have obtained a quantitative description of villin-nucleated actin polymerization in physiological salt by determining the concentrations of free villin (V), villin–actin monomer (VA), villin–actin dimer (VA_2), and villin–actin oligomer (VA_n). Over a range of actin–villin ratios from 0.1 to 20 we determined the concentration of actin-bound villin by measuring the *low*-intensity pyrenylactin fluorescence of the two terminal actins in each villin–actin polymer. (To this end we first showed that each villin–actin oligomer and polymer contains two low-intensity pyrenylactin molecules.) We determined the concentration of free villin using a calibrated cutting activity assay. The pattern of increase in bound villin together with the pattern of increase in *high*-intensity pyrenylactin fluorescence with increasing G-actin concentration indicated, first, that villin–actin monomers were not formed at detectable levels even at a 12-fold villin excess over actin. Second, there was no stoichiometric villin–actin dimer formation at actin–villin ratios of 2. Instead there was an equilibrium between free villin, VA_2, and VA_n. Defining $K_1 = [VA]/[V][A]$ and $K_2 = [VA_2]/[VA][A]$, a good fit of the data was obtained with $K_1 \ll K_2$ and a value of $K_1K_2 = K_V = 10^{12}$–10^{13} $M^{-2} = [VA_2]/[V][A]^2$, i.e., $1/K_V^{1/2} = (0.3\text{–}1) \times 10^{-6}$ M. We have assumed here that the monomer binding constant of VA_2 to form VA_3 was equal to the monomer binding constant of pointed filament ends, $K_\infty = 1/c_\infty$, obtained as described below. Extending polymerization measurements to actin–villin ratios greater than 100 showed that F-actin increased gradually with increasing G-actin concentrations until a limiting value for the G-actin concentration was obtained, c_∞, approaching $1/K_\infty$ for the pointed filament end. The data could be fitted with the same three constants, K_1, K_2, and K_∞, used for the data in the low range of actin–villin ratios. Retaining the term critical concentration for the limiting G-actin concentration during nucleated polymerization, F-actin is formed at subcritical actin concentrations. In other words, filament assembly no longer has the characteristics of condensation polymerization but instead is described by a series of equilibria that are very similar to those derived by Oosawa for the analogous case of "linear" polymerization.

Actin filaments in nonmuscle cells probably are repeatedly assembled and disassembled to adapt to different functions. Filament formation and breakdown appears to be regulated by actin binding proteins, a large number of which have been isolated [for reviews, see Korn (1982), Craig and Pollard (1982), Weeds (1982), Stossel et al. (1985), and Pollard and Cooper (1986)]. These proteins are capable of bundling filaments, nucleating the formation of new filaments, stabilizing the filaments by capping both ends, or assisting in filament disassembly by stabilization of monomeric actin (G-actin), by filament breakage, and by capping of the preferred end for elongation (Wegner, 1976; Kirschner, 1980).

At this time relatively little is known about the participation of these proteins in intracellular processes. In vitro studies,

† This work was supported by NIH Grants HLB 15585 (Pennsylvania Muscle Institute) (J.N. and A.W.) and AM 25387 (M.S.M.) and March of Dimes Basic Research Grant 1-924 (M.S.M.).
* Author to whom correspondence should be addressed.
‡ University of Pennsylvania.
§ Drexel University.
‖ Present address: Department of Physics, Virginia Commonwealth University, Richmond, VA 23284.
⊥ Yale University.

0006-2960/87/0426-2528$01.50/0

meanwhile, are providing information on how these proteins can function. We have focused on studies of villin, a specialized protein found only in microvilli of the intestines and kidney [for a review, see Mooseker (1985)]. Whereas nothing is known about its function in vivo, a number of different properties have been determined by in vitro studies [cf. Mooseker (1985)]. In the presence of calcium, villin caps, nucleates, and cuts actin filaments. Although villin has these activities in common with gelsolin, fragmin, and severin (Wang & Bryan, 1981; Bryan & Coluccio, 1985; Hasegawa et al., 1979; Hinssen et al., 1981a,b; Brown et al., 1982; Yamamoto et al., 1982), there are considerable differences between villin and these other proteins concerning the detailed regulation of these functions. For instance, while all villin functions are rapidly reversed in response to calcium addition or removal, the capping activity of gelsolin and severin is not reversed by the subsequent removal of calcium, even though calcium appears to be required initially for the activation of these proteins (Bryan & Kurth, 1984; Bryan & Coluccio, 1985; Janmey et al., 1985; Yamamoto et al., 1982).

Recently (Walsh et al., 1984a,b; Northrop et al., 1986), we began a study of the quantitative aspects of the interactions between villin and actin. We determined that different calcium levels are required for the regulation of cutting and capping so that the calcium sensitivity of cutting is 4 orders of magnitude lower than that of capping. We showed that villin binds to the barbed end with an association constant of about 10^{11} M^{-1} and to cutting sites with a much lower affinity. We provided evidence to indicate that the energy required to break the actin–actin bonds during cutting may be derived from the difference in binding energy of villin to the capping and to the cutting sites.

Here we present a detailed analysis of the nucleation of actin polymerization by villin in physiological salt solutions. Nucleating activity is defined in terms of the relative concentrations of villin–actin monomers, dimers, and oligomers of increasing size coexisting with free villin and G-actin. We employed several independent methods to measure the concentrations of free villin and G-actin and the number concentrations of total actin–villin oligomers. We found, first, that the villin–actin dimer was never the sole villin–actin species but always coexisted with larger villin–actin oligomers and free villin. Second, we found that the concentration of the villin–actin monomers was always negligible even at very low actin–villin ratios. Third, we found that the equilibria (or steady states) between the various villin–actin species could be described by three apparent equilibrium constants, K_1, K_2 and $K_\infty = 1/c_\infty$, whereby $K_1 \ll K_2$ and $(K_1K_2)^{1/2} = K_V^{1/2} \sim K_\infty$. We show that, as a consequence of the high value for K_V, filament assembly by villin was no longer described by condensation polymerization characteristic of pure actin. Instead, it followed a linear reaction scheme, analogous to that derived by Oosawa for "linear" polymerization [cf. Oosawa and Asakura (1976)]. It could be described by the three constants derived from the measurements described above, whereby $(K_1K_2)^{1/2}$ is equivalent to Oosawa's equilibrium constant for actin dimer formation.

Experimental Procedures

Actin Preparations. Actin was prepared from acetone powder and chromatographed as previously described (Walsh et al., 1984a). Chromatography by downward flow through Bio-Gel P-150 separated the unidentified substance with nucleating activity, present in actin extracts, quite well when the column was freshly poured; on repeated use, however, the nucleating activity tended to spread deeper and deeper into the actin fractions, a problem that was recently overcome by changing to upward flow. Unmodified actin was stored in liquid nitrogen over long periods of time. Chromatographed actin used for experiments was kept for 2–4 weeks at 4 °C in a column buffer containing 5 mM triethanolamine, pH 7.5, 0.5 mM ATP, 0.2 mM $CaCl_2$, 0.1 mM CaEDTA,[1] and 6 mM NaN_3 (G buffer).

Actin modified with *N*-ethylmaleimide or NBD was prepared as previously described (Porter & Weber, 1979; Detmers et al., 1981). Pyrenylactin was prepared according to Kouyama and Mihashi (1981) with the following modification. After removal of dithiothreitol by overnight dialysis, actin was brought to a final concentration of 40 μM in G buffer with 10 mM Tris-HCl, pH 8.0, and the following additions were made in sequence: first, $MgCl_2$ to a final concentration of 2.0 mM; second, pyrenyliodoacetamide, dropwise under stirring, to a final concentration of 45 μM from a 2.5 mM stock solution in dimethyl sulfoxide; third, KCl to a final concentration of 0.1 M. After 90-min incubation at 15 °C, actin was centrifuged for 2 h at 100000*g*, dialyzed against G buffer containing Tris-HCl, pH 8.0, and chromatographed. Addition of magnesium prior to pyrenyliodoacetamide resulted in greater reproducibility of the fluorescence response of the modified actin, which usually showed a 30-fold increase on polymerization. When first used in our laboratory, labeling by this method was found to be more than 90% as measured by subsequent labeling with *N*-ethylmaleimide. The extent of labeling, however, was not tested for each preparation. The critical concentration was determined for each preparation as previously described (Walsh et al., 1984a); it varied between 0.1 and 0.2 μM when both filament ends were free and between 0.7 and 1.2 μM when the barbed ends were fully capped by villin.

Villin was prepared according to Coleman and Mooseker (1985) and stored for several weeks at 4 °C. Fresh dithiothreitol was added to a concentration of 0.1 mM once a week. Changes in the activity of villin with time were followed by titrating 3 μM actin with villin to find the villin–actin ratio at which the increase in the steady-state monomer concentration was maximal, i.e., the fluorescence increment was lowest. With fresh villin this was usually at an actin–villin ratio of about 1/800. Villin was rejected when the ratio had increased to 1/600.

Protein concentrations for villin and actin were calculated from $E_{280} = 123.5$ mM^{-1} cm^{-1} for villin and $E_{290} = 24.9$ mM^{-1} cm^{-1} for actin. The concentration of pyrenylactin was corrected for the absorption of the probe according to Selden and colleagues (Selden et al., 1983).

Fluorescence and Kinetic Measurements. Fluorescence measurements were carried out as previously described (Walsh et al., 1984a): excitation–emission wavelengths were 360–410 nm for pyrenylactin and 470–530 nm for NBD-actin. Light scattering artifacts were minimized by 390- and 490-nm cut-off filters in the emission path for pyrenylactin and NBD-actin, respectively. The highest concentration of pyrenylactin used was 1.4 μM, calculated to permit 95% transmission after polymerization, with $E_{370} = 0.016$ μM^{-1} cm^{-1} for F-actin. The fraction of fluorescent-labeled actin used in different experiments varied and is given in the legend of each figure.

Experiments were carried out at 14 °C in polymerizing buffer containing 0.5 mM ATP, 10 mM Tris-HCl, pH 7.4 or

[1] Abbreviations: EGTA, ethylene glycol bis(β-aminoethyl ether)-*N*,*N*,*N*′,*N*′-tetraacetic acid; NEM, *N*-ethylmaleimide; NBD-Cl, 7-chloro-4-nitro-2,1,3-benzoxadiazole; VA_n, villin–actin oligomers with *n* actin molecules per villin; EDTA, ethylenediaminetetraacetic acid; Tris-HCl, tris(hydroxymethyl)aminomethane hydrochloride.

7.6, 2.0 mM $MgCl_2$, 0.1 M KCl, and $CaCl_2$ as indicated for each experiment. Prior to polymerization, G-actin was converted to Mg-actin; i.e., the tightly bound calcium was exchanged for magnesium. This was done to avoid the change in elongation rates associated with the conversion of calcium to magnesium monomers (Cooper et al., 1983; Frieden, 1983; Selden et al., 1983; Tobacman & Korn, 1983) and to study actin filaments in their physiological state, since calcium- and magnesium-containing filaments differ significantly in some properties (Brenner & Korn, 1984). The exchange was carried out a short time before polymerization, since we observed a decrease in the extent of polymerization on prolonged storage of G-actin in magnesium. Godette et al. (1986) very recently elucidated the mechanism of this apparent instability of magnesium actin. The exchange procedure consisted of a 15-min incubation at 14 °C in magnesium exchange solution containing 10 mM imidazole or Tris-HCl, pH 7.6, EGTA equivalent to the calcium present, and varying magnesium concentrations dependent on the ATP concentrations used. At ATP concentrations between 100 and 300 μM, the total magnesium was 100 μM higher than that of ATP; at 500 μM ATP, the total magnesium concentration was 500 μM. The conversion to Mg-actin was indicated by a small drop in the pyrenyl fluorescence.

Villin-capped actin oligomers and polymers were polymerized 18–24 h prior to use in the presence of 0.1 M KCl and 2.0 mM $MgCl_2$ and 200 μM calcium; concentrations of actin varied between 1 and 10 μM and of villin between 1.0 and 19 μM. For the determination of the critical concentration (c_∞), the polymerized actin was allowed to reach steady state at 16–19 °C for a period of 18 h. ATP was not significantly depleted during 24 h since the steady-state rate of ATP hydrolysis by actin present as villin-capped actin filaments (average length 100 monomers/villin) at 14 °C was about (4–5) $\times 10^{-5}$ M ATP/M actin per second (Chaparala et al., submitted for publication); i.e., maximally 50 μM ATP was hydrolyzed by 10 μM actin during 24 h. Nevertheless, in a number of experiments we supplemented the assays with 5 mM creatine phosphate and 0.1 mg/mL creatine phosphokinase. No difference was observed between assays with and without the ATP backup system (Table I, Figure 5).

Determination of Free Villin Present in Villin–Actin Oligomer Mixtures by Its Cutting Ability. Three requirements must be met to use this assay. The number of cuts per villin molecule must be constant over the range of villin concentrations to be measured. Second, the number of cuts made per villin molecule must be known; i.e., the cutting activity of the particular villin preparation must be calibrated under the given experimental conditions. Third, the starting concentration of the filaments must be known. The third requirement was met by using, as a substrate for cutting, villin-capped actin filaments of an average size of 600 molecules per villin, prepared by polymerizing 7–9 μM actin in the presence of villin at a ratio of total actin to villin of 600. For the cutting assays (Northrop et al., 1986) the villin-capped actin filaments (6 μM actin) were incubated (in the presence of 1.0 mM $CaCl_2$) either with a known concentration of free villin (20–70 nM) for the calibration or with the villin–actin mixtures to be analyzed. After incubation periods of varying lengths but not shorter than 90 s, the cutting activity of villin was terminated by dilution of the actin filaments into an EGTA-containing (6.0 mM) polymerizing solution to a final actin concentration of 50–80 nM. The extent of cutting was evaluated from the rate of depolymerization. At each step, mixing and sample transfer was very slow to minimize filament shearing. The first fluorescence reading was taken about 20–30 s after dilution of the villin–actin mixture to subcritical actin concentrations.

The extent of cutting was calculated (see below) from the depolymerization rate. The extent of cutting was the same for incubation periods from 2 to 20 min, indicating that the cutting process had reached an end point at less than 2 min, i.e., before the assay was terminated, confirming earlier results (Northrop et al., 1986). The depolymerization rates of control filaments, not subjected to cutting, were measured after the same mechanical procedures, substituting villin buffer for villin. After some practice runs, the control rates were very reproducible. The calculation of the number concentration of cuts per villin was based on the premise that under the conditions chosen the depolymerization rate was proportional to the number concentration of the filaments. This has been verified for average filament lengths (after cutting) down to, but not below, 100 monomers per filament (Northrop et al., 1986). The number concentration of cuts per assay is given by $q = (i_v/i_c - 1) f_0$, where i_c and i_v are depolymerization rates before and after cutting by villin and f_0 is the number concentration of actin filaments before cutting.

The number of cuts per villin molecule did not change over the measured range of villin concentrations from 20 to 170 nM. Its value, q_v, varied for different villin preparations between 0.18 and 0.5. The free villin present in the villin–actin oligomers was given by q/q_v, where q is the number concentration of cuts made by the villin–actin oligomer mixture.

The observation that the number of cuts per villin was smaller than the number of filaments produced by villin-nucleated polymerization may be explained in one of two ways. First, it is possible that cutting and nucleating activity are not equally susceptible to inactivation. It has been our impression, not yet verified by a systematic study, that the cutting activity is more labile than the nucleating or the capping activity. Second, there may have been competition between villin binding alongside the actin filaments (resulting in cutting of the filament) and villin interacting with actin monomers to form villin–actin nuclei. Elongation of villin–actin dimers and trimers to longer oligomers measurable by depolymerization tests should take much longer than the cutting times used here. The reason is that the diffusional processes responsible for the redistribution of actin molecules from preformed filaments to the villin–actin nuclei would be very slow (Hill). Thus, the filament number remained constant for about 20 min after the initial rapid increase after villin addition although it was found to have increased after 24 h.

Calculations. (*A*) *Calculation of G- and F-Actin Concentrations from Fluorescence Data for Figures 2 and 3.* Concentrations of G- and F-actin (total polymerized actin) were calculated according to the following expression: emission = a[G-actin] + b[F-actin], where [G-actin] = [total actin] − [F-actin]. This was rearranged to [F-actin] = (emission − a[total actin])/($b - a$), where a is the molar fluorescence of G-actin, determined under the ionic conditions prevailing in the mixture of G- and F-actin during the experiment, and b is the molar fluorescence of F-actin, obtained from the slope of F-actin fluorescence.

(*B*) *Model for Assembly.* We employed a simple linear model for the binding of villin to actin, with an equilibrium constant K_1 for the binding of the first actin to villin, an equilibrium constant K_V for the binding of two actin monomers to villin, and an equilibrium constant K_∞ for the binding of a monomer to a villin-capped actin filament containing two or more actin molecules per villin. This is a simple modifi-

cation of the "linear polymerization" described by Oosawa [cf. Oosawa and Asakura (1976)].

Using the mass action law, the concentrations $[VA_n]$ of n actin monomers bound to villin are given by

$$[VA] = K_1VG \quad (1a)$$

$$[VA_2] = K_VVG^2 \quad (1b)$$

$$[VA_n] = K_\infty[VA_{n-1}]G = (K_VVG^2)(K_\infty G)^{n-2} \quad \text{for } n > 2 \quad (1c)$$

where V is the free villin concentration and G is the G-actin concentration. The total concentration of bound villin V_{bd} is the sum of all the $[VA_n]$:

$$V_{bd} = [VA] + [VA_2] + [VA_3] + \ldots = V_t[K_1G + (K_V - K_1K_\infty)G^2]/[1 + (K_1 - K_\infty)G + (K_V - K_1K_\infty)G^2] \quad (2)$$

where V_t is the total villin concentration. The free villin concentration is

$$V = V_t - V_{bd} = V_t(1 - K_\infty G)/[1 + (K_1 - K_\infty)G + (K_V - K_1K_\infty)G^2] \quad (3)$$

This permits calculation of the concentrations of oligomers of each size, $[VA_n]$, given the total villin concentration. If c_0 is the total concentration of actin molecules, then the total concentration of monomers incorporated into villin–actin complexes is

$$F = c_0 - G = [VA] + 2[VA_2] + 3[VA_3] + \ldots = VG[K_1 + K_VG(2 - K_\infty G)]/[(1 - K_\infty G)^2] \quad (4)$$

The data are normalized by dividing the number concentration of filaments by the total villin concentration. Substituting eq 3 for V then gives

$$F/V_t = [G/(1 - K_\infty G)][K_1(1 - K_\infty G)^2 + K_VG(2 - K_\infty G)]/[1 + (K_1 - K_\infty)G + (K_V - K_1K_\infty)G^2] \quad (5)$$

The appropriate equations were fit to the data with a nonlinear least-squares procedure that employs a Marquardt algorithm [cf. Bevington (1969)]. The standard error of the parameter is found by inverting the curvature matrix, choosing the diagonal element of this inverse that corresponds to the parameter of interest, and multiplying this by the square root of the reduced χ^2. The choice of this method for determining the standard error was in part motivated to allow for comparisons to popular routines, such as those of MLAB (Knott & Shrager, 1972).

Results

Polymerization of Actin in the Presence of Stable Nuclei. The simplest and most direct measurement of the effect of a nucleating substance, such as villin, on actin polymerization is to determine the partition of the total actin into F- and G-actin. Figure 1 shows a control experiment with pure actin in the absence of villin. Data points were clustered in the region of actin concentrations near the critical concentration c_∞. A sharp break can clearly be seen between the two linear regions of the plot of fluorescence against total actin. The abruptness of the transition is typical for condensation–polymerization and is the result of the low concentration of F-actin at subcritical levels (Oosawa & Kasai, 1962), which was too small to be detected with the methods employed here, although more sensitive techniques may have rendered it observable [Lanni & Ware, 1984; Newman et al., 1985; but compare Godette et al. (1986)].

In the presence of villin two features of the polymerization curve were altered. First, the critical concentration (the extrapolation of the linear part of the curve to the abscissa) was raised to the value for the pointed end. This is due to the complete block by villin of monomer binding and dissociation at the pointed end. Second, the total observed fluorescence increased with a gradually increasing slope, which eventually reached a constant value at higher actin concentrations (Figure 2). This gradual increase in slope is not related to the shift in critical concentration. If the monomer binding constant were the same at both filament ends, as in the case of ADP-actin in the absence of ATP, then the gradual increase in slope would have occurred without any change in critical concentration.

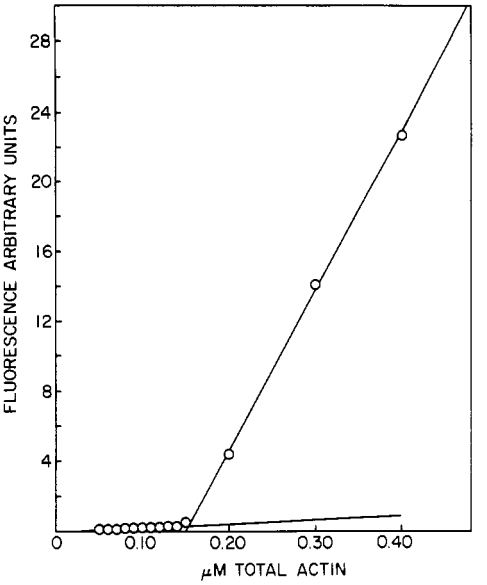

FIGURE 1: Absence of measurable amounts of actin oligomers at subcritical actin concentrations in the absence of added nuclei. Pyrenylactin:NEM-actin = 1:1.

This gradual increase in fluorescence was seen both with native actin (Figure 2A) and with NEM-NBD-actin (Figure 2B) and became more obvious with higher villin concentrations (Figure 2A). It was less noticeable with NBD fluorescence, first, because of the much lower sensitivity of this probe and, second, because the VA_2–F-actin fluorescence ratio was much higher for NBD-actin than for pyrenylactin (see below and Figure 4). The gradual increase in slope indicates that initially both F- and G-actin increased together until the G-actin concentration reached a maximal value where it remained constant. At that point, raising the concentration of total actin further only resulted in an increase of the concentration of F-actin (Figure 3A). The value at which the G-actin concentration remained constant was independent of the villin concentration.

As the concentration of villin increased, the amount of F-actin formed at submaximal G-actin concentrations also increased. However, the ratio of bound actin over total villin at a given monomer concentration was independent of the villin concentration (Figure 3B). This would be expected for a series of equilibria (or steady states) between villin–actin complexes of increasing size:

$$V + A \leftrightarrow VA + A \leftrightarrow VA_2 + A \leftrightarrow VA_3 + A \leftrightarrow \ldots \leftrightarrow VA_{n-1} + A \leftrightarrow VA_n$$

At an actin–villin ratio between 10 and 20, the concentration of G-actin reached its maximal value, which we define as the critical concentration (c_∞) for the pointed end because it approximates $1/K_\infty$ for monomer binding to the pointed end (Oosawa & Asakura, 1973).

To obtain the line through the data points of Figure 3, the simplifying assumption was made that, except for villin and

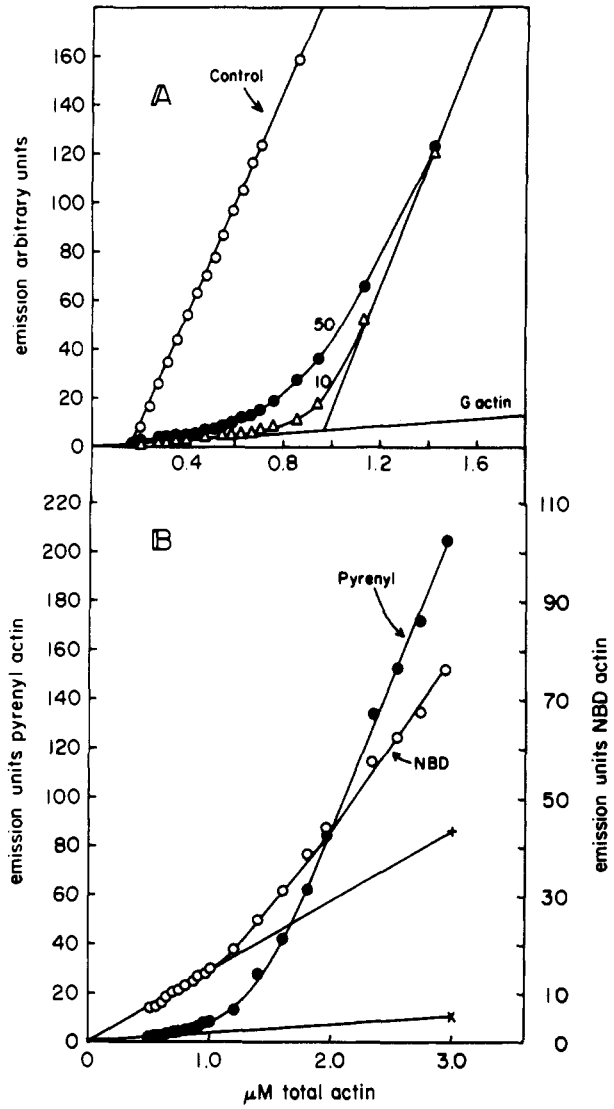

FIGURE 2: Fluorescence with increasing actin in the presence of a constant villin concentration. (A) Native actin containing 20% pyrenylactin; villin concentrations in nanomolar indicated on curves; control, villin absent. (B) With 7 nM villin, 1:3 pyrenylactin:NBD-actin.

Table I: Equilibrium Constants Used to Fit the Data Showing the Increase of F-Actin at Increasing Subcritical G-Actin for Different Actin and Villin Preparations

data set	c_∞ (μM)	K_∞ (μM^{-1})	K_1 (μM^{-1})	K_V (μM^{-2})
3/18	0.94	1.06 ± 0.01	0.0 ± 0.7	2.5 ± 0.6
4/12	1.19	0.84 ± 0.04	0.0 ± 2.4	3.5 ± 3.0
4/19	1.28	0.78 ± 0.01	0.0 ± 0.6	1.1 ± 0.2
5/10	1.07	0.93 ± 0.02	0.0 ± 1.2	1.2 ± 0.4
6/24[a]	0.83	1.20 ± 0.01	0.0 ± 0.7	0.9 ± 0.4

[a] With 5.0 mM creatine phosphate and 0.1 mg/mL creatine phosphokinase NP.

the villin–actin monomer, VA, all villin–actin oligomers had the same binding constant, $K_\infty = 1/c_\infty$. The curve was calculated by least-squares fitting the data of Figure 3B to eq 5 (cf. Experimental Procedures). As can be seen, the data are well described by the fit, with reproducible and stable values obtained for the fitted parameters (Table I). Two results emerge: first, a sizable fraction of the villin is predicted to be unbound (over 50% at the lowest measured value of G-actin), and second, the binding constant for the first monomer is too small to be determined with precision by this procedure. These results were checked by direct measurements of free villin and villin–actin oligomers with several independent

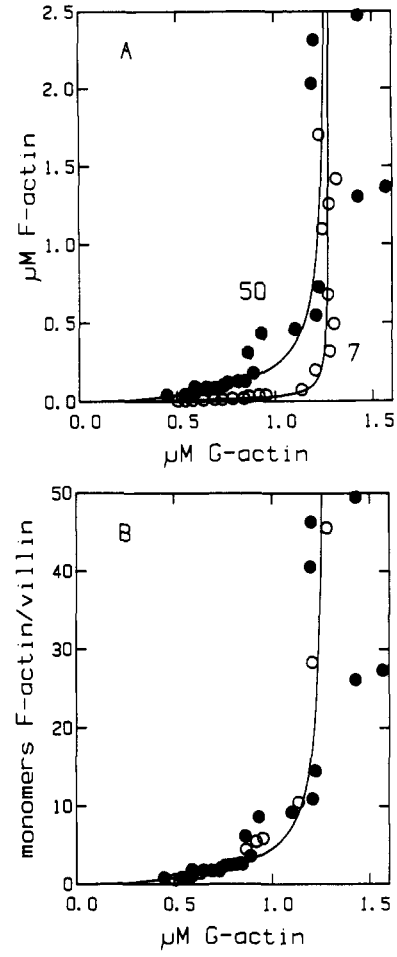

FIGURE 3: Increase in polymerized and monomeric actin with increasing total actin at 7 and 50 nM villin; data with 7 nM villin were calculated from the fluorescence values in Figure 2B. (A) Increase in total F-actin; (B) data in (A) expressed as ratio of polymerized actin over total villin; 1:3 pyrenylactin:NBD-actin. Curves in both (A) and (B) were calculated from eq 5 (Experimental Procedures) with $K_V = 1.1 \times 10^{12}$ M^{-2}, $K_1 = 0$, and $K_\infty = 0.78$ μM^{-1}.

methods at low actin–villin ratios.

Formation of the Villin–Actin Dimer. The formation of the villin–actin dimer, $V + A \leftrightarrow VA + A \leftrightarrow VA_2$, represents the first two steps in the linear reaction scheme describing villin-nucleated polymerization. The two steps can be combined to give the expression $K_V = K_1K_2 = [VA_2]/(G^2V)$. To obtain a precise value for K_V, the concentrations of monomeric actin, G, free villin, V, and the villin–actin dimer, $[VA_2]$, must be determined. We measured the concentration of monomeric actin by a null point method that will be described below. The determination of free villin and of the villin–actin dimers is more difficult because under most conditions, for example, at an actin–villin ratio of 2, villin–actin dimers, unlike gelsolin–actin dimers (Bryan & Kurth, 1983; Janmey et al., 1985, 1986; Coué & Korn, 1985), coexisted with free villin and villin–actin oligomers of larger size. Without specific markers for each, we could not distinguish between VA, VA_2, and VA_n. However, we did measure free villin directly by its cutting ability and the total number concentration of villin–actin oligomers by two different methods.

In the following we describe, step by step, first, the determination of G-actin, second, the evidence suggesting that each villin–actin oligomer and polymer contains two low-intensity molecules, and, third, the determination of free villin by its cutting activity. Fourth, from the last two measurements together, we determine that VA did not occur in significant concentrations even at the lowest actin–villin ratios used. Fifth,

Table II: Determination of the Steady-State Monomer Concentration during Polymerization[a]

[actin] (μM)	[villin] (μM)	actin–villin ratio	c_0 (nM)	ΔF/min (arbitrary units)
1.0	2.0	0.5	51	−0.29
			203	0.0
			406	+0.5
2.0	2.0	1.0	152	−0.1
			254	+0.07
			406	+0.19
2.0	1.0	2.0	102	−0.43
			209	−0.06
			305	0.0
			609	+1.1
3.0	1.0	3.0	305	−0.2
			495	0.0
			711	+1.16

[a] Actin was polymerized with villin for 18 h at different actin–villin ratios (columns 1–3); aliquots were diluted to 40 nM total villin into G-actin (c) of increasing concentrations. Simultaneously, $MgCl_2$ was added to 2.0 mM, KCl to 0.1 M, and $CaCl_2$ to 0.2 mM. The fluorescence change of NBD-actin, ΔF/min, was measured in arbitrary units. A rate of zero indicates that the fluorescence did not change after dilution for a period of 10 min. It should be noted that elongation rates are not linear functions of the monomer concentration (Weber et al., 1987).

we are then in a position to determine how the number concentration of villin–actin oligomers increased with increasing F-actin–villin ratios and extract a value for K_V by best fit of the data with the linear reaction scheme used for fitting the data of Figures 2 and 3.

Determination of G-Actin Concentrations. We determined the monomer concentration by a null-point method. Steady-state villin–actin oligomers of different average sizes were diluted into various G-actin solutions: if the concentration of the G-actin solution was not equal to the steady-state value for the particular mixture of villin–actin oligomers, then the villin–actin oligomers either depolymerized or elongated; if it was the same, no change occurred. A representative example of these determinations is given in Table II. The values for the G-actin concentrations at the null point were verified with NBD-actin, since Carlier and her colleagues (Carlier et al., 1984) have shown that the fluorescence of NBD-actin is insensitive to the nucleotide content (ATP vs. ADP) of F-actin. By contrast, the fluorescence of pyrenylactin is lower for F-ATP-actin than for F-ADP-actin. The same null-point values were obtained with both fluorescent probes (data not shown), indicating that no changes in nucleotide content occurred.

The steady-state G-actin concentration was much lower than c_∞ at low actin–villin ratios; it was 0.05 μM at a ratio of 0.08, the lowest ratio employed. The reason is that at these low ratios the G-actin concentration depended on $G = \{[VA_2]/(VK_V)\}^{1/2}$. The G-actin concentration increased with increasing villin–actin ratios, reaching the value of c_∞ at an F-actin–total villin ratio between 10 and 20. At this higher ratio the controlling factor for the monomer concentration became k_-/k_+ of the pointed filament ends, since with decreasing values of V the value of k_-/k_+ eventually became lower than that of $\{[VA_2]/(VK_V)\}^{1/2}$. The value of c_∞ was determined from the linear part of a graph of fluorescence vs. total actin (Figure 2).

Determination of the Number Concentration of Villin–Actin Oligomers and Polymers Using the Low Fluorescence Intensity of Two Pyrenylactin Molecules in Each Villin–Actin Complex. The fluorescence of actin bound to short villin-capped oligomers was much lower than that of F-ADP-actin in long

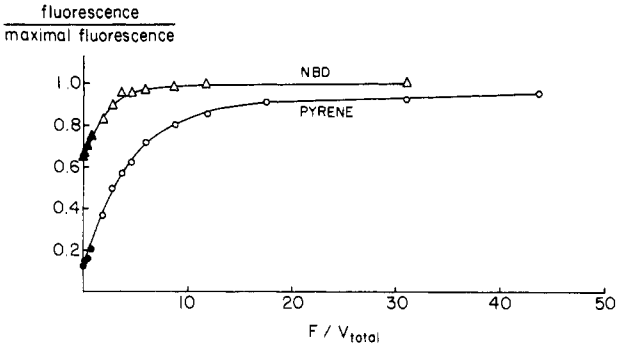

FIGURE 4: Increase in the fluorescence of villin-bound actin with increasing F-actin–villin ratio. The data were normalized by dividing the observed fluorescence values by that of an equivalent concentration of F-ADP-actin in long filaments, obtained from the linear slope of measurements shown in Figures 1 and 2. This means that the ordinate shows fluorescence as a fraction of b (Experimental Procedures). The numerator in the ordinate refers to total fluorescence minus that of G-actin, and F on the abscissa designates total actin minus G-actin. These corrections were small since the G-actin concentration was never more than 10% of the total actin. The solid line was drawn by eye through the data points. (Open symbols) 10 μM total actin (NBD-actin:pyrenylactin:NEM-actin = 1:1:3) was incubated with increasing villin for 18 h without creatine phosphate and creatine phosphokinase. (Closed symbols) Different villin and actin preparations: 1.5–2.0 μM total actin, 5.0 mM creatine phosphate, and 0.1 mg/mL creatine phosphokinase; highest villin concentration 12 μM; pyrenylactin:NBD-actin:NEM-actin = 1:1:1.

filaments (Figure 4). For example, at the lowest ratio of F-actin to total villin, the pyrenyl fluorescence was only about 12% of that of F-ADP-actin or 4 times that of G-actin. This value is somewhat higher than that observed for gelsolin-bound actin in actin–gelsolin mixtures with a ratio of 2 (Harris & Weeds, 1983; Janmey et al., 1985; Coué & Korn, 1986). The total fluorescence increased with increasing length of the villin-capped filaments, i.e., increasing F-actin–villin ratio, and it approached the value for F-ADP-actin at an average length greater than 100 monomers per villin (data not shown).

The continued increase in fluorescence over such a large range of actin–villin ratios suggested that each villin–actin oligomer and polymer contained one or more actin molecules of low fluorescence intensity. By contrast, if low-intensity molecules existed only in villin–actin dimers and trimers and if in larger polymers their fluorescence intensity were switched to the normal fluorescence values of F-ADP-actin inside a polymer, then pyrenyl fluorescence would have reached its limiting value at much lower F-actin–villin ratios.[2]

The number of low fluorescence actin molecules in each villin–actin oligomer was obtained from the data in Figure 4, by the following calculations. We made the plausible assumption that each filament contained only two classes of fluorescent molecules: normal, high-intensity F-ADP-actin and a new low-intensity species. We related the ordinate of Figure 4, i.e., the observed F-actin fluorescence divided by the maximal fluorescence of an equivalent concentration of F-ADP-actin free of villin (viz., at large values of F/V_t), to the concentration F_{li} of bound low-intensity molecules:

$$em' = [em - aG]/(bF) = [a'F_{li} + b(F - F_{li})]/(bF) \quad (6)$$

where em′ is the ordinate in Figure 4, em is the total fluorescence and a, a', and b are the molar fluorescences of

[2] For instance, NBD fluorescence reached a limiting value at relatively low actin–villin ratios (Figure 4). However, the resolution of NBD fluorescence was too low to draw the conclusion that NBD fluorescence of a villin-bound actin molecule may have switched to the normal intensity of NBD–F-actin in larger villin–actin oligomers.

Table III: Number of Low-Intensity Molecules per Oligomer Obtained from Fluorescence and Cutting Data

F/V_t	F_{li}/V_t	V_{bd}/V_t	F_{li}/V_{bd}
0.5	0.45	0.17	2.0
1.0	0.87	0.25	3.5
1.0	0.35		2.4
2.0	1.4	0.45	3.0
2.0	0.7		2.0
2.5	1.6	0.65	2.4
0.75	2.0		
5	2.0		
10	2.0		
15	1.9		
20	2.0		

G-actin, low-intensity F-actin, and normal F-actin, respectively. For large F-actin–villin ratios, F_{li} becomes insignificant compared with F. In the limit of very small F/V_t, essentially all bound-actin molecules have low fluorescence, so that $F_{li} = F$ and $em' = a'/b = 0.12$ (the intercept of the pyrene curve with the ordinate in Figure 4). This yielded the value of a', which was otherwise unknown.

The total concentration of low-intensity bound actin was obtained by rearranging eq 9 (see below) to give

$$F_{li} = F(1 - em')/(1 - a'/b) \quad (7)$$

The number of low-intensity molecules for each polymer was then found by dividing F_{li} by the number concentration of villin–actin oligomers, i.e., the concentration V_{bd} of bound villin. [Note that V_{bd} approaches V_t at high actin–villin ratios when each villin molecule nucleates one filament (Northrop et al., 1986; Coleman & Mooseker, 1985).]

A simple procedure for obtaining F_{li}/V_{bd} is illustrated in Table III. Column 1 gives the values of F/V_t for the data points in Figure 4. Column 2 gives F_{li}/V_t, obtained from eq 7. In column 3 are values of V_{bd}/V_t, obtained from direct measurement of free villin by its cutting activity. Cutting was measured by its effect on depolymerization rates after dilution of the filaments to subcritical actin concentrations (Northrop et al., 1986; cf. Experimental Procedures). The concentration of free villin was calculated by comparing the total number of cuts made by the actin–villin mixture with the calibrated cutting activity of the villin preparation used for the experiment. These measured free villin concentrations, converted to bound villin = total villin − free villin and normalized for total villin, are listed in column 3. The number of low-intensity molecules per villin–actin oligomer, F_{li}/V_{bd}, shown in column 4, was obtained by dividing column 2 by column 3. The number shows considerable scatter due to the technical difficulty of these experiments, and the mean value is somewhat greater than 2. Since even at very small $F-V_t$ ratios two or more low-intensity actin molecules per bound villin were found, VA must constitute an insignificant fraction of the bound villin. In other words, the number concentration of villin–actin oligomers and polymers is at most equal to half the concentration of bound low-intensity actin molecules. However, in view of the rather large scatter of the data, it is important that the fluorescence data themselves provide an independent confirmation of the insignificance of VA.

That there are two low-intensity molecules per oligomer is also suggested by the lower third of column 2 in Table III, where at F/V_t greater than 5 F_{li}/V_t may be considered equal to F_{li}/V_{bd} [i.e., virtually all villin is bound; cf. also Figure 5 in Weber et al. (1987)]. The number two is plausible because it corresponds on the one hand to the number of terminal actin molecules bound to villin and on the other to the number of actin molecules in a special position at the filament end.

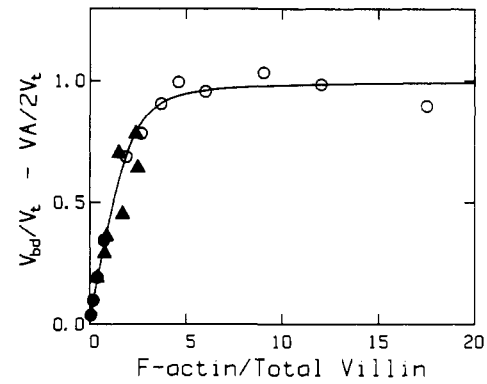

FIGURE 5: Increase in actin-bound villin with increasing actin–villin ratio was calculated for each data point in Figure 4 as outlined under Results. Open and closed circles are the result of data points from Figure 4 substituted into the right-hand side of eq 9; closed triangles are data points obtained from determinations of free villin by its cutting activity as described under Results; 5.0 mM creatine phosphate and 0.1 mg/mL creatine phosphokinase. The solid curve was calculated from eq 10 (ordinate) and eq 5 (abscissa) with $K_V = 6.9 \times 10^{12}$ M^{-2}, $K_1 = 0$, and $K_\infty = 1.0$ μM^{-1}.

It is not necessary to employ the cutting data to conclude that the concentration of VA is insignificant and to determine the binding constant K_V of villin to the first two monomers on the barbed end. The decreasing fluorescence with decreasing values of F/V_t (i.e., decreasing lengths of filaments) itself provides a direct way of determining the concentration of bound villin. That is, if all villin were bound, then the data in Figure 4 would lie on a horizontal line. To begin this analysis, the fluorescence emission (em) must be written in terms of the following contributions from [VA], [VA_2], and F (total bound actin):

$$em = a'([VA] + 2[VA_2]) + b(F - [VA] - 2[VA_2]) \quad (8)$$

where two bound actins per oligomer were assumed to be of low intensity. We then normalized em by bF to obtain em', wrote [VA_2] in terms of V_{bd} and [VA], and rearranged eq 8 in such a way that [VA] and V_{bd}, the unknown quantities, are on the left-hand side of the equation, and em' and F, the measured quantities, are on the right-hand side of the equation:

$$V_{bd}/V_t - [VA]/(2V_t) = (em' - 1)(F/V_t)/[2(a'/b - 1)] \quad (9)$$

We then substituted values of em' and F/V_t from Figure 4 on the right-hand side of eq 9 to obtain the measured values for $V_{bd}/V_t - [VA]/(2V_t)$ vs. F/V_t, which are plotted as open and closed circles in Figure 5. After this conversion we fit these data points (solid line in Figure 5) by the following procedure. For increasing concentrations of G-actin (determined as described above), the values for total F-actin/total villin (abscissa) were derived from eq 5 (Experimental Procedures), and the values for $V_{bd}/V_t - [VA]/(2V_t)$ were calculated according to the following expression, which was obtained from eq 1 and 2 (Experimental Procedures):

$$V_{bd}/V_t - [VA]/(2V_t) = [K_1G + G^2(K_V - K_1K_\infty)]/[1 + (K_1 - K_\infty)G + (K_V - K_1K_\infty)G^2] \quad (10)$$

The value obtained for K_V by this fitting procedure was 6.9 ± 4.5 μM^{-2} ($K_\infty = 1.0$ μM^{-1}), while K_1 was indistinguishable from zero. This is consistent with the observation from Figure 5 that, at an actin–villin ratio of 2, about 30% of the villin was still free, indicating the coexistence of villin–actin dimers with a significant fraction of larger oligomers. It also confirms the conclusions of both the cutting data and the analysis of Figures 1 and 2 that VA constituted an insignificant fraction of the solution. Since [VA] is practically zero, the ordinate in Figure

5 is essentially V_{bd}/V_t, and so we plotted the cutting data as solid triangles on the same graph in order to show agreement with the fluorescence data.

Discussion

The major result of this study is a determination of the nucleating activity of villin in terms of the relative concentrations of villin–actin monomers, dimers, and oligomers at low actin–villin ratios. Relevant for the nucleating activity are the following observations. First, villin–actin monomers did not exist in significant concentrations even when villin was present in 10-fold excess over actin. Second, the villin–actin dimer always coexisted with longer villin–actin oligomers and free villin. These conclusions are based on direct observations from a variety of experiments and are independent of any modeling. The relationships between the various villin–actin species are defined by the relative values of K_1 and K_2, i.e., $K_1 \ll K_2$, and by the ratio of $K_V^{1/2}$ to K_∞, which was between 1 and 3. The further conclusion that the apparent affinity of the monomer for the villin–actin dimer is the same as that for the pointed end is based on best fit of the data modeled with this assumption.

A value of 10^{12}–10^{13} M^{-2} for K_V is consistent with the value for the binding constant of villin to filament ends K_b = 10^{11}–10^{12} M^{-1} determined previously (Walsh et al., 1984a; Northrop et al., 1986). With $K_V^{1/2} = (1–3) \times 10^6$ M^{-1} and $K_\infty = 1 \times 10^6$ M^{-1} at higher actin–villin ratios, practically all villin forms villin–actin oligomers larger than VA_2, and very little villin remains free or bound to actin monomers or dimers. This conclusion is confirmed by electron microscopic measurements of average filament length at actin–villin ratios of 100 or more, showing one filament per villin (Coleman & Mooseker, 1985; Northrop et al., 1986).

Last, in view of the concerns of one of the reviewers, it should be emphasized that the treatment in terms of three equilibrium constants can be equally applied to a set of coupled equilibria and a set of intermediates at steady state. The constants in either case can be written as k_+/k_-. This is true so long as the concentration of the intermediates remains constant. Thus under most conditions, the steady-state behavior of actin in the presence of ATP is accurately described by a single constant, $K_\infty = 1/c_\infty$, even though there is ATP hydrolysis and treadmilling. That the thermodynamic meaning of the constants is quite different in the two cases is not relevant to this presentation.

Since the confidence in the equilibrium constant for villin–actin dimer formation, K_V, depends on the quality of the measurements of G-actin, free villin, and villin–actin oligomers, we discuss in the following some of the experimental difficulties and their resolution. Experimentally most sensitive were the null-point determinations of steady-state monomer concentrations at low actin–villin ratios; most accurate was the measurement of the concentration of the bound low-intensity actin molecules, which directly gave the number concentration of the villin–actin oligomers. [It is not known whether all dimers and barbed filament ends contain two low-intensity actin molecules or whether the quenching of the fluorescence is the result of capping by villin or gelsolin (Harris & Weeds, 1983; Janmey et al., 1985; Coué & Korn, 1985).]

The values for free villin obtained from the cutting assay are not subject to two potential errors that can be associated with this assay. First, dissociation of villin from villin–actin oligomers after dilution into the cutting assay was prevented by the high monomer concentration in the assay. Second, a decrease in free villin by binding to actin monomers, which were present in a higher concentration in the cutting assay than in the villin–actin mixture to be tested, was canceled out by the calibration procedure.

Villin may form villin–actin dimers in preference over villin–actin monomers for one of two reasons. First, the concentration of actin monomers may be very low even in the absence of villin if the protomer of magnesium actin should be the dimer rather than the monomer. The latter has been suggested by Pardee and his colleagues (Pardee et al., 1982) but disagrees with the modeling of nucleation data by Frieden (1983) and appears to be ruled out by the recent findings by Godette and Frieden (1986). If in addition villin, like gelsolin, has two actin binding sites (Janmey et al., 1985), then the concentration of VA may be quite negligible (energy square I). Matsudaira (personal communication) has obtained evidence suggesting that villin has four actin binding sites.

The second possibility to consider (energy square II) is that, while in the absence of villin, actin dimer formation is very unfavorable [as suggested by Frieden (1983)], the binding of the second actin to villin is cooperative. Such a cooperativity has been observed for gelsolin–actin binding at low salt (Coué & Korn, 1985, 1986; Janmey et al., 1986], although it is not clear whether this is also the case in physiological salt solutions [compare Janmey et al. (1985) with Coué and Korn (1985)].

The difference between the two mechanisms is most easily visualized by energy squares. Their use may be justified in

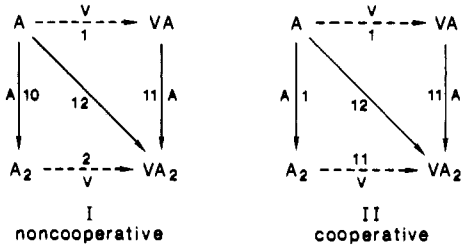

spite of the ATPase activity of actin because Mockrin and Korn (1983) have shown that covalently cross-linked actin dimers still contain ATP as their bound nucleotide and Coué and Korn (1986a) have shown the same for the gelsolin–actin dimer.

The numbers on the arrows are the decadic logarithms of the equilibrium constants for the reactions described by the arrows. The diagonal represents villin–actin dimer formation from actin monomers and villin, with log K_V = 12, and the two clockwise arrows subdivide this reaction into the two steps discussed above with log K_1 and log K_2. The counterclockwise arrows show the second pathway for VA_2 formation, actin dimer formation followed by villin binding to the dimers with log K_D and log (K_1K_3), whereby K_1 and K_3 describe actin binding by each of the two putative actin binding sites on villin. It can be seen that for the noncooperative mechanism (energy square I) each actin binding site on villin has the same binding constant for actin ($K_1K_3 = 10^2$; $K_3 = K_1 = 10^1$). In this case monomer binding to VA is so much stronger than monomer binding to villin because the actin–actin dimer bond in itself is so strong. $K_2 > K_D$ because the second monomer binds to the second site on villin in addition to forming a dimer with the first villin-bound actin. For the cooperative mechanism, the second monomer binds much more strongly to villin than does the first, whereas the actin–actin dimer bond remains weak. At this point there are no data that allow a distinction to be made between the two mechanisms.

As a consequence of the high equilibrium constant for villin–actin dimer formation, filament assembly no longer shows the characteristics of condensation polymerization. Instead, it is described by a linear polymerization scheme

governed by the same three equilibrium constants that were derived from the measurements made at low actin–villin ratios. Nucleated polymerization differs from linear polymerization treated by Oosawa [cf. Oosawa and Asakura (1976)] only in terms of two parameters: the fixed concentration of nucleating substance and the resulting greater number of equilibrium constants. The equilibrium constant describing actin dimer formation in the "linear" polymerization scheme is equivalent to $K_V^{1/2}$, since K_V contains the equilibrium constant for villin binding to the actin dimer (cf. energy squares, counterclockwise arrows). Nucleated polymerization presumably describes filament assembly under physiological conditions since cells possess many nucleating centers, and therefore, condensation polymerization would not be expected to occur.

ACKNOWLEDGMENTS

We are very grateful to Clara Franzini-Armstrong for the electron microscopy of actin filaments. We thank Frank Tilli for the preparation and quality control of the actin preparations. We are indebted to Joseph Bryan for his critical reading of the manuscript and for stimulating discussions.

REFERENCES

Bevington, P. R. (1969) *Data Reduction and Error Analysis for the Physical Sciences*, pp 204–246, McGraw-Hill, New York.

Brenner, S. L., & Korn, E. D. (1984) *J. Biol. Chem. 259*, 1441–1446.

Brown, S. S., Yamamoto, K., & Spudich, J. A. (1982) *J. Cell Biol. 93*, 205–210.

Bryan, J., & Kurth, M. C. (1984) *J. Biol. Chem. 259*, 7480–7487.

Bryan, J., & Coluccio, L. M. (1985) *J. Cell Biol. 101*, 1236–1244.

Carlier, M. F., Pantaloni, D., & Korn, E. D. (1984) *J. Biol. Chem. 259*, 9983–9986.

Coleman, T. R., & Mooseker, M. S. (1985) *J. Cell Biol. 101*, 1850–1857.

Cooper, J. A., Buhle, E. L., Walker, S. B., Tsong, T. X., & Pollard, T. D. (1983) *Biochemistry 22*, 2193–2202.

Coué, M., & Korn, E. D. (1985) *J. Biol. Chem. 260*, 15033–15041.

Coué, M., & Korn, E. D. (1986) *J. Biol. Chem. 261*, 1588–1593.

Craig, S. W., & Pollard, T. D. (1982) *Trends Biochem. Sci. (Pers. Ed.) 7*, 88–92.

Detmers, P., Weber, A., Elzinger, M., & Stephens, R. E. (1981) *J. Biol. Chem. 256*, 99–105.

Frieden, C. (1983) *Proc. Natl. Acad. Sci. U.S.A. 80*, 6513–6517.

Glenney, J. R., & Weber, K. (1981) *Proc. Natl. Acad. Sci. U.S.A. 78*, 2810–2814.

Glenney, J. R., Geisler, N., Kaulfus, P., & Weber, K. (1981) *J. Biol. Chem. 257*, 8156–8161.

Godette, D. W., Uberbacher, E. C., Bunick, G. J., & Frieden, C. (1986) *J. Biol. Chem. 261*, 2605–2609.

Hasegawa, T., Takahayashi, H., & Hatano, S. (1979) *Biochemistry 18*, 2677–2683.

Hinssen, H. (1981a) *Eur. J. Cell Biol. 23*, 225–233.

Hinssen, H. (1981b) *Eur. J. Cell Biol. 23*, 234–240.

Janmey, P. A., Chaponnier, C., Lind, S. E., Zaner, K. S., Stossel, T. P., & Yin, H. L. (1985) *Biochemistry 24*, 3714–3723.

Kirschner, M. W. (1980) *J. Cell Biol. 86*, 330–334.

Knott, G. D., & Shrager, R. I. (1972) *Comput. Graph.: Proc. SIGGRAPH Comput. Med. Symp. ACM, SIGGRAPH Not. 6*, 138–151.

Korn, E. D. (1982) *Physiol. Rev. 62*, 672–737.

Kouyama, T., & Mihashi, K. (1981) *Eur. J. Biochem. 114*, 33–38.

Lanni, F., & Ware, B. R. (1984) *Biophys. J. 46*, 97–110.

Matsudaira, P., Jakes, R., & Walker, J. E. (1985) *Nature (London) 315*, 248–250.

Mockrin, S. C., & Korn, E. D. (1983) *J. Biol. Chem. 258*, 3215–3221.

Mooseker, M. S. (1985) *Annu. Rev. Cell Biol. 1*, 261–293.

Newman, J., Esters, J. E., Selden, L. A., & Gershman, L. C. (1985) *Biochemistry 24*, 1538–1544.

Northrop, J., Weber, A., Mooseker, M. S., Armstrong, C., Bishop, M. F., Dubyak, G. R., Tucker, M., & Walsh, T. P. (1986) *J. Biol. Chem. 261*, 9274–9281.

Oosawa, F., & Kasai, M. (1962) *J. Mol. Biol. 4*, 10–21.

Oosawa, F., & Asakura, S. (1975) *Thermodynamics of the Polymerization of Proteins*, Academic, New York.

Pantaloni, D., Carlier, M. F., Coué, M., Lal, A. A., & Brenner, S. L. (1984) *J. Biol. Chem. 259*, 6274–6283.

Pardee, J. D., Reidler, J., Stryer, L., & Spudich, J. J. (1982) *Biophys. J. 37*, 40a (Abstr.).

Pollard, T. D., & Cooper, J. A. (1986) *Annu. Rev. Biochem. 55*, 987–1035.

Porter, M., & Weber, A. (1979) *FEBS Lett. 105*, 259–262.

Selden, L. A., Estes, J. E., & Gershman, L. C. (1983) *Biochem. Biophys. Res. Commun. 116*, 478–485.

Tobacman, L. S., & Korn, E. D. (1983) *J. Biol. Chem. 258*, 3207–3214.

Walsh, T. P., Weber, A., Higgins, J., Bonder, E. M., & Mooseker, M. S. (1984a) *Biochemistry 23*, 2613–2621.

Walsh, T. P., Weber, A., Davis, K., Bonder, E., & Mooseker, M. S. (1984b) *Biochemistry 23*, 6099–6102.

Wang, L. L., & Bryan, J. (1981) *Cell (Cambridge, Mass.) 25*, 637–649.

Weber, A., Northrop, J., Bishop, M. F., Ferrone, F. A., & Mooseker, M. S. (1987) *Biochemistry* (following paper in this issue).

Weeds, A. (1982) *Nature (London) 296*, 811–816.

Wegner, A. (1976) *J. Mol. Biol. 108*, 139–150.

Yamamoto, K., Pardee, J. D., Reider, J., Stryer, L., & Spudich, J. A. (1982) *J. Cell Biol. 95*, 711–719.